

International Conference on Space Optics—ICSO 2010

Rhodes Island, Greece

4–8 October 2010

*Edited by Errico Armandillo, Bruno Cugny,
and Nikos Karafolas*



How nonlinear optics can merge interferometry for high resolution imaging

D. Ceus, F. Reynaud, A. Tonello, L. Delage, et al.



International Conference on Space Optics — ICSO 2010, edited by Errico Armandillo, Bruno Cugny, Nikos Karafolas, Proc. of SPIE Vol. 10565, 105652H · © 2010 ESA and CNES
CCC code: 0277-786X/17/\$18 · doi: 10.1117/12.2309204

HOW NONLINEAR OPTICS CAN MERGE INTERFEROMETRY FOR HIGH RESOLUTION IMAGING

Speaker: D. Ceus

Co-authors: F. Reynaud, A. Tonello, L. Delage, L. Grossard.

¹Xlim Département photonique, France.

I. INTRODUCTION

High resolution stellar interferometers are very powerful efficient instruments to get a better knowledge of our Universe through the spatial coherence analysis of the light. For this purpose, the optical fields collected by each telescope T_i are mixed together. From the interferometric pattern, two expected information called the contrast C_{ij} and the phase information φ_{ij} are extracted. These information lead to the V_{ij} , called the complex visibility, with $V_{ij}=C_{ij}\exp(j\varphi_{ij})$. For each telescope doublet T_iT_j , it is possible to get a complex visibility V_{ij} . The Zernike Van Cittert theorem gives a relationship between the intensity distribution of the object observed and the complex visibility. The combination of the acquired complex visibilities and a reconstruction algorithm allows imaging reconstruction.

To avoid lots of technical difficulties related to infrared optics (components transmission, thermal noises, thermal cooling...), our team proposes to explore the possibility of using nonlinear optical techniques. This is a promising alternative detection technique for detecting infrared optical signals. This way, we experimentally demonstrate that frequency conversion does not result in additional bias on the interferometric data supplied by a stellar interferometer.

In this presentation, we report on wavelength conversion of the light collected by each telescope from the infrared domain to the visible. The interferometric pattern is observed in the visible domain with our, so called, upconversion interferometer. Thereby, one can benefit from mature optical components mainly used in optical telecommunications (waveguide, coupler, multiplexer...) and efficient low-noise detection schemes up to the single-photon counting level.

II. TEST PRINCIPLES AND RESULTS

In this part we describe our experimental setup. First, we give a description of a high resolution angular interferometer, then our experimental configuration is described, and finally, we report on the experimental result achieved until nowadays.

A. Description

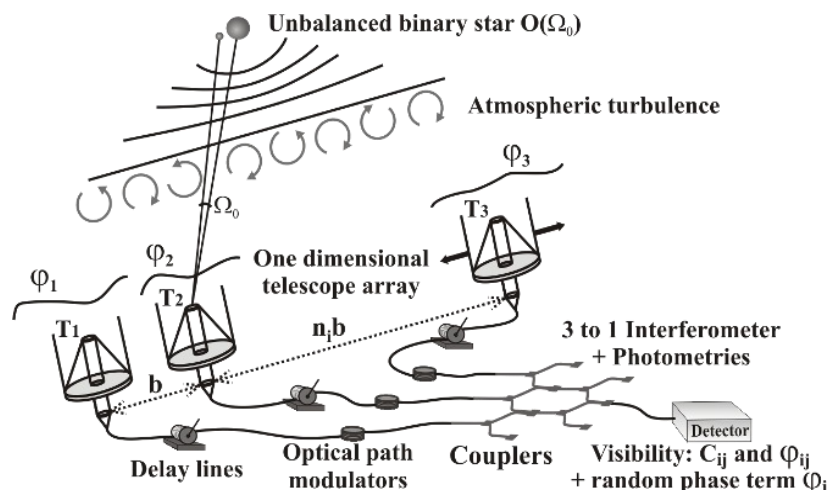


Fig. 1. Global scheme of a high resolution stellar interferometer.

Fig. 1 shows the principle of a one-dimension telescope array able to provide high resolution images for optical astronomy. The object under test have a spatial angular intensity distribution called $O(\Omega)$. The baseline T_1T_2 (i.e the distance between T_1 and T_2) is fixed and equal to b . The distance T_2T_3 can be set to $n_i b$ with n_i an integer. The Zernike Van Cittert theorem gives the relation between the theoretical complex visibility $V(n_i, b)$ and the spatial angular intensity distribution $O(\Omega)$:

$$V(n_i, b) = 1/I \int_{Object} O(\Omega) \exp(2\pi j n_i b \Omega / \lambda_{IR}) d\Omega \quad (1)$$

where λ_{IR} is the mean wavelength of the analyzed radiation and I the total intensity emitted by the object. Equation (1) shows that the theoretical fringe visibility is equal to the spatial angular Fourier Transform of the spatial angular intensity distribution: $V(n_i, b) = (I/I_0)\tilde{O}(N_i)$ where $N_i = n_i b / \lambda_{IR}$ is the i -th spatial frequency. The complex visibility contains all the information needed for imaging reconstruction. To validate the conservation of the optical properties of the object under test, we laboratory demonstrated that the complex visibility remains unchanged after frequency conversion from infrared light to visible light. For this purpose, different experimental setups were achieved. The first one was dedicated to the conservation of the contrast [1]. The second experimental setup describes the use of the phase closure technique applied to our upconversion interferometer [2].

B. Experimental setup

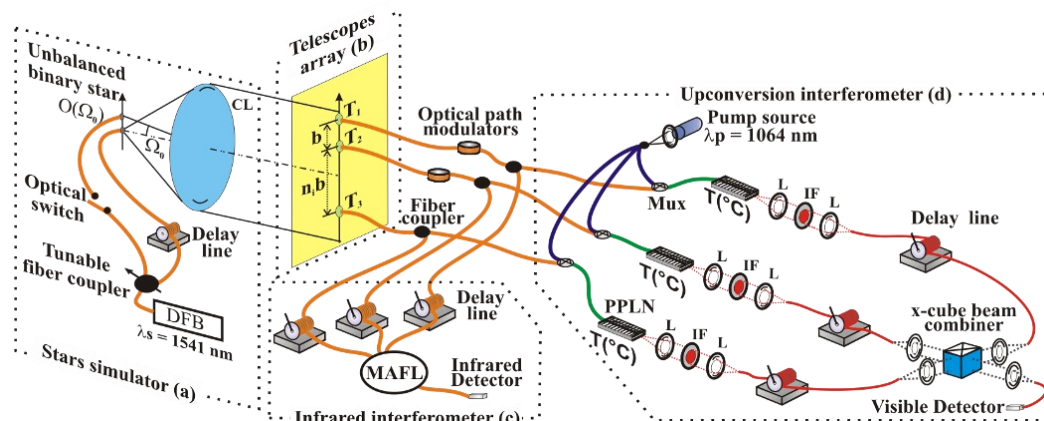


Fig. 2. Experimental setup of the upconversion interferometer test bench. DFB : Distributed Feed Back laser at 1541 nm, CL : Collimating Lens, $n_i b$ the baseline between a couple of telescopes $T_i T_j$ with n_i an integer, Mux : allows the combination of the signals at 1541 nm and 1064 nm, PPLN : Periodically Poled Niobate Lithium, MAFL : Multi-Aperture Fiber Linked Interferometer, $T(^{\circ}C)$: temperature controller, IF : Interference Filter at $\lambda = 630 \text{ nm} \pm 20 \text{ nm}$, L : Lens. The delay lines are used for precision optical path length control in the infrared and visible interferometers.

In our test-bench, the object to be imaged was an unbalanced laboratory binary star. For this purpose, a 1 to 2 fiber coupler with a μ adjustable splitting ratio allowed to route the optical light emitted by a distributed feed back laser (DFB) ($\lambda_{IR} = 1541 \text{ nm}$). The two fiber outputs acted as point-like sources spaced by $27.9 \mu\text{m}$. The first coupler output was used directly as point-like source. To ensure the spatial incoherence of this binary star, a fiber delay line of 500 m length was inserted in the second path, to induce an optical path difference longer than the 100 m coherence length of the DFB laser. The two fiber-ends were placed in the focal plane of a collimating lens with a 1900 mm focal length and a 190 mm diameter. The resulting characteristics of our laboratory object corresponded to a binary star with an $\Omega_0 = 14.7 \mu\text{rad}$ angular separation and an adjustable intensity ratio (μ). Each telescope T_i was composed of an achromatic doublet ($f = 10 \text{ mm}$). $T_1 T_2$ was fixed and spaced by a $b = 16 \text{ mm}$ separation. T_3 was moved by steps equal to $n_i b$.

The optical fields, picked at each telescope focus, fed single mode optical fibers used as interferometric arms. Different optical path modulations have been applied on each interferometric arm in order to display the interferometric signal in the time domain. The Fourier Transform of this interferometric signal was composed of three frequencies related to the three couples of telescopes. On each arm, a fiber coupler allowed to send 90% of the optical beam to our upconversion interferometer. The remaining 10% are routed to a classical infrared interferometer previously developed by our team for the Multi Aperture Fiber Linked Interferometer (MAFL) project [3] (bottom left Fig.2). Due to its demonstrated accuracy and calibration, the MAFL has been used as a reference in this experimental work.

In the upconversion interferometer, the nonlinear frequency conversion was performed in each interferometric arm using PPLN waveguides with an $11.3 \mu\text{m}$ poling periodicity.

In about 40 mm long Ti-indiffused waveguides the signal radiation was mixed with a narrow-band pump at 1064 nm in order to generate a sum frequency signal at nearly 630 nm. Each upconverted signal passed through an interference filter to block residual pump radiation and then fed a single mode fiber at 630 nm. In each arm, the optical fields were combined together with a double beam splitter in an X configuration (X-cube). This device had 4 inputs and 4 outputs. In our experimental configuration, it had been used as a symmetrical 3 to 1 coupler

for the visible radiation mixing. This massive component was very stable over time and allowed to get our data with a good accuracy. The beam out-going from the X-cube was sent to a silicon avalanche photodiode. The raw data were analyzed to extract phase closures and contrasts. In a first stage, the two interferometers were calibrated with a point-like source. In such a configuration, the contrasts and the phase closure are theoretically equal to 1 and 0 respectively. For this purpose, one of the two “stars” had been switched off. The very small instrumental offset on phase closure was corrected for both interferometers in order to get visible and infrared calibrated measurements.

C. Contrast conservation

The expression of the contrast for a binary star could be derived as:

$$C_{ij} = \sqrt{\left[1 + \mu \cos\left(\frac{n_i b}{\lambda} \cdot \theta_0\right)\right]^2 + \left[\mu \sin\left(\frac{n_i b}{\lambda} \cdot \theta_0\right)\right]^2}$$

As we can see, C_{ij} is a function of the baseline $n_i b$, which is defined as the distance between two telescopes T_i and T_j . C_{ij} is obtained with our upconversion interferometer. For this purpose, the tunable fiber coupler is adjusted to get an equilibrated binary star. Then, we used different configurations of the telescope array to extract the contrast from the interferometric signal. Fig.3 represents the C_{ij} as a function of the normalized baseline. Dot line plots the theoretical data, the crosses plot the infrared data, and diamonds the visible one. As we can see, there is a very good agreement between all the data, and we check the conservation of the contrast using our optical interferometer.

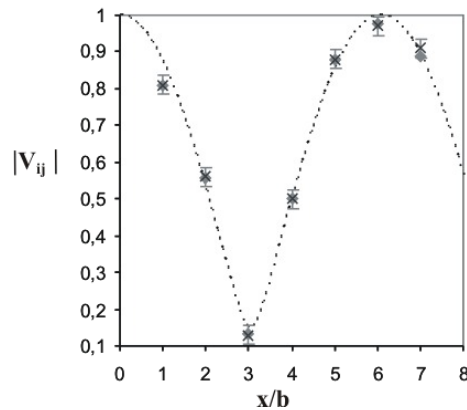


Fig. 3. Experimentally measured fringe contrast obtained from the upconversion (diamonds) and from the infrared interferometer (crosses).

D. Phase information conservation

In a second stage, we had to check the conservation of the phase information by using our upconversion interferometer. Unfortunately, atmospheric turbulence and/or instrument instabilities (particularly in space mission) induce random phase shifts on the visibility function. Consequently, a direct measurement of the phase of the complex visibility, ϕ_{ij} , is quite impossible. To overcome this limitation, Jennison proposed the use of the phase closure technique [4]. The phase closure term is theoretically unaffected by atmospheric turbulences or instruments instabilities, and allows image reconstruction [5]. This technique can be implemented only with a three (or more) arm interferometer. The theoretical expression of the phase closure for a three-telescope-array is derived as:

$$\Phi = \arctan\left[\frac{\mu \sin\left(\frac{n_1 b}{\lambda} \cdot \theta_0\right)}{1 + \mu \cos\left(\frac{n_1 b}{\lambda} \cdot \theta_0\right)}\right] + \arctan\left[\frac{\mu \sin\left(\frac{n_2 b}{\lambda} \cdot \theta_0\right)}{1 + \mu \cos\left(\frac{n_2 b}{\lambda} \cdot \theta_0\right)}\right] + \arctan\left[\frac{\mu \sin\left(\frac{n_3 b}{\lambda} \cdot \theta_0\right)}{1 + \mu \cos\left(\frac{n_3 b}{\lambda} \cdot \theta_0\right)}\right]$$

With $n_1 b$ the baseline between $T_1 T_2$, $n_2 b$ linked to $T_2 T_3$ and $n_3 b$ to $T_1 T_3$. We can see that Φ is a function of the photometric ratio of the binary star μ , which depends on the source tuneable fibre coupler. After the same calibration used before to get the contrast, we recorded the phase closure term for different values of μ (variable binary star). These measurements were compared with simulated data and with the infrared reference interferometer as shown in Fig.4 (next page). The following curve reports the phase closure as function of the μ

parameter. Dot line is the theoretical data, plus plots the infrared data, and crosses the visible one. The error bars are not plotted for an easier comprehension, but they are less than 25 mrad . As we can see there is a very good agreement between all the data. This demonstrates the conservation of the phase information, through the phase closure term, using our optical interferometer.

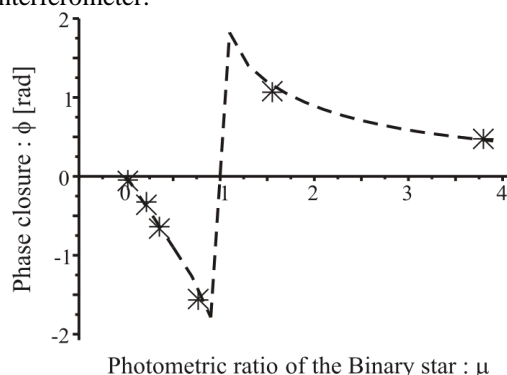


Fig. 4. Phase closure measurements as function of μ with a telescope array configuration $n_1=1$, $n_2=2$ and $n_3=3$. + plots the infrared data, and X the visible one. Dash line reports the theoretical simulation data.

Fig. 5 gives an overview of our experimental setup used for both contrast and phase closure retrieving after a stage of frequency conversion from infrared to visible wavelength.

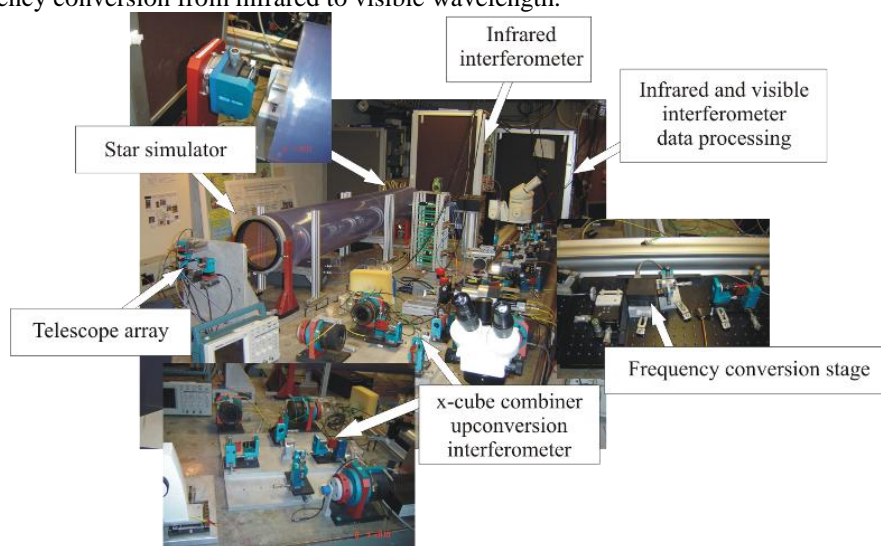


Fig. 5. Overview of the experimental setup.

III. PROSPECTS

The next step of our experimental investigation will be to operate our upconversion interferometer for aperture synthesis (acquisition of both phase and contrast information) at low power levels, down to the photon counting regime. We also plan to broaden the spectral bandwidth and to improve our conversion efficiency.

REFERENCES

- [1] S. Brutlein, L. Del Rio, A. Tonello, L. Delage, F. Reynaud, "Laboratory Demonstration of an infrared-to-visible up-conversion interferometer for spatial coherence analysis," *Phys. Rev. Lett.*, Vol. 100 pp.153903-1-153903-4, April 2008.
- [2] D. Ceus, A. Tonello, L. Delage, F. Reynaud, H. Herrmann and W. Sohler, "Phase Closure Retrieval in an Infrared-to-Visible Upconversion Interferometer for High Resolution Astronomical Imaging", submitted for publication in PRL.
- [3] S. Olivier *et al.* "MAFL experiment: development of photonic devices for a space-based multiaperture fiber-linked interferometer", *Appl. Opt.*, pp. 46:834, February 2007.
- [4] R. C. Jennison *et al.* *R. Astron. Soc.*, 3:276, February 1958.
- [5] G. Huss, F. Reynaud, and L. Delage. "All guided three-arm interferometer for stellar interferometry" *Opt. Commun.*, 196:55, September 2001.